HHS Public Access

Author manuscript

J Acoust Soc Am. Author manuscript; available in PMC 2019 December 26.

Published in final edited form as:

J Acoust Soc Am. 2012 February ; 131(2): 1605–1612. doi:10.1121/1.3672701.

Relationships of quantitative ultrasound parameters with cancellous bone microstructure in human calcaneus *in vitro*.

Keith A. Wear, **Srinidhi Nagaraja**, **Maureen L. Dreher**

U.S. Food and Drug Administration, Center for Devices and Radiological Health, 10903 New Hampshire blvd., Silver Spring, MD 20993

Sheng L. Gibson

National Institute of Standards and Technology, 100 Bureau Drive, Gaithersburg, MD 20899

Abstract

Ultrasound parameters (attenuation, phase velocity, and backscatter), bone mineral density (BMD), and microarchitectural features were measured on 29 human cancellous calcaneus samples *in vitro*. Regression analysis was performed to predict ultrasound parameters from BMD and microarchitectural features. The best univariate predictors of the ultrasound parameters were the indexes of bone quantity: BMD and bone volume fraction (BV/TV). The most predictive univariate models for attenuation, phase velocity, and backscatter coefficient yielded adjusted squared correlation coefficients of 0.69 – 0.73. Multiple regression models yielded adjusted correlation coefficients of 0.74 – 0.83. Therefore, attenuation, phase velocity, and backscatter are primarily determined by bone quantity, but multiple regression models based on bone quantity plus microarchitectural features achieve slightly better predictive performance than models based on bone quantity alone.

Keywords

quantitative ultrasound; cancellous bone; microstructure; bone mineral density

I. INTRODUCTION

Because of low cost, portability, and lack of ionizing radiation, quantitative ultrasound is an attractive alternative to x-ray bone densitometry for the assessment of osteoporotic fracture risk (Langton *et al.*, 1984;Laugier, 2008; Laugier, 2011; Barkmann and Glüer, 2011). A recent position paper by the International Society for Clinical Densitometry indicates growing acceptance of quantitative ultrasound (Krieg *et al.*, 2008).

It is well understood that fracture risk depends not only on BMD (the current gold standard diagnostic measurement) but also on structural properties of the bone. Correlative studies involving quantitative ultrasound measurements and micro computed tomography (microCT) measurements on cancellous bone samples provide insight into relationships

Corresponding author: Keith A. Wear, Food and Drug Administration, Center for Devices and Radiological Health, Bldg. 62, Room 3108, 10903 New Hampshire blvd., Silver Spring, MD 20993, (301) 796-2538, keith.wear@fda.hhs.gov.

between macroscopic ultrasound properties and microarchitectural features. Previous regression studies have been conducted in human calcaneus (Nicholson *et al.*, 2001;Chaffai *et al.*, 2002;Wear and Laib, 2003), tibia and femur (Hakulinen *et al.*, 2006;Karjalainen *et al.*, 2009), and femur (Padilla *et al.*, 2008). The literature in this area of investigation was recently reviewed thoroughly by Padilla *et al.* (2008). These studies were based on linear regression analysis, which is the most straightforward approach when the true functional dependencies of the output variables (e.g., ultrasound properties) on the input variables (e.g., BMD and microarchitectural features) are unknown.

This paper reports multiple regression analysis to predict quantitative ultrasound parameters from BMD and microarchitectural measurements in 29 human cancellous calcaneus samples *in vitro*. This analysis provides insight into determinants of clinical ultrasound measurements. The calcaneus is important because it is the most common bone measured by clinical bone sonometers.

The contributions of this paper are as follows. 1) This paper reports multiple regression analysis to predict broadband ultrasonic attenuation and phase velocity as functions of BMD and microarchitecture in human calcaneus and provides independent data to compare with similar human calcaneus studies reported previously by Nicholson *et al.* (2001) and Chaffai *et al.* (2002). 2) This paper reports measurements of relationships between ultrasound backscatter, BMD, and micro-architecture in human calcaneus and investigates the degree of reproducibility of similar studies reported previously only by Chaffai *et al.* (2002) and Wear and Laib (2003). (The latter study utilized a different set of bone samples than the set reported in the present paper and only considered mean trabecular thickness but not other microarchitectural features such as bone volume fraction and mean trabecular number). 3) This paper provides an analysis of the range of values of correlation coefficients among ultrasound parameters, BMD, and microarchitectural features reported in this study and previous studies on human cancellous bone (Nicholson *et al.*, 1998;Trebacz and Natali, 1999;Nicholson *et al.*, 2001;Chaffai *et al.*, 2002;Hakulinen *et al.*, 2006;Padilla *et al.*, 2008;Karjalainen *et al.*, 2009).

II. METHODS

A. Bone samples

Twenty-nine excised human calcaneus samples (extracted from 29 human calcanei) were defatted using a trichloro-ethylene solution. According to previous studies, defatting has a small effect on ultrasound parameters (Langton *et al.*, 1996;Alves *et al.*, 1996;Njeh and Langton, 1997;Nicholson and Bouxsein, 2002;Hoffmeister *et al.*, 2002). The lateral cortical layers were sliced off leaving two parallel surfaces with direct access to trabecular bone. Cortical end-plates have been reported to have a small but measureable (15%) effect on measurements of broadband ultrasound attenuation (Xia *et al.*, 2005). A thin layer of cortical bone remained along the other surfaces of the bone. This cortical layer (see periphery of bone sample in Figure 1) was excluded from regions of interest for bone densitometry, microCT, and ultrasound measurements. The mean sample thickness was 1.8 cm (standard deviation = 0.23 cm).

B. Bone Densitometry

Bone mineral density (BMD) was measured using a Hologic QDR 4500 dual energy x-ray absorptiometry (DXA) system operating in single beam mode. Areal density was determined for central regions of interest (ROIs) so that cortical bone was excluded. The ROIs were approximately 1.8 cm × 3.6 cm × 1.8 cm (where the last dimension corresponds to the bone sample thickness, which is in the direction parallel to the DXA beam and perpendicular to the plane of Figure 1). Duplicate measurements (without repositioning) were performed on each specimen. The average coefficient of variation for the duplicate areal density determinations was 1.6%. The average areal density (g/cm^2) was divided by the thickness of each sample to give volumetric density (g/cm^3).

C. MicroCT

Three-dimensional (3-D) trabecular bone microstructure was measured using micro computed tomography (μCT 100, Scanco Medical, Basserdorf, Switzerland). The Scanco μCT 100 is a cabinet cone-beam scanner with a microfocus x-ray source and a charge coupled device detector (3072 × 400 elements array). After ultrasound and DXA measurements had been performed, cancellous bone specimens were cut down to dimensions approximately 2.0 cm × 4.0 cm × 1.8 cm and imaged at an isotropic voxel size of 17.2 μm (nominal resolution). This resolution has been reported to be sufficient to reveal significant differences between normal and osteoporotic human trabecular bone for bone volume fraction (BV/TV), trabecular thickness (Tb.Th), degree of anisotropy (DA), trabecular number (Tb.N), trabecular spacing (Tb.Sp), and structural model index (SMI) (Isaksson *et al.*, 2011). Within the 2.0 cm × 4.0 cm × 1.8 cm reconstruction volume, an interior volume, approximately 1.8 cm × 3.6 cm × 1.6 cm (similar to the DXA analysis volume) was delineated for micro-structural analysis. A constant threshold to distinguish trabecular bone from background was chosen through histogram analysis of each specimen. The threshold was designated at a value below the broad peak in the histogram corresponding to trabeculae. From these segmented images, automated distance transformation algorithms were used to calculate BV/TV, Tb.Th, Tb.Sp, Tb.N, SMI, bone surface fraction (BS/BV), and connectivity density (Conn.D.) based on methods of Hildebrand and Ruegsegger (Ruegsegger *et al.*, 1996;Hildebrand and Ruegsegger, 1997;Hildebrand *et al.*, 1999). Principal material orientations (H1, H2, and H3) and degree of anisotropy (DA) were calculated using 3-D mean intercept length techniques.

D. Ultrasound

Prior to ultrasonic interrogation, samples were vacuum degassed underwater in a desiccator. Subsequently, samples were allowed to thermally equilibrate to room temperature. Water temperature was measured with a digital thermometer for each experiment and ranged between 19°C and 21°C. The relative orientation between the ultrasound beam and the calcaneus samples was the same as with *in vivo* measurements performed with commercial bone sonometers, in which sound propagates in the mediolateral (or lateromedial) direction. Samples were interrogated in a water tank using a Panametrics (Waltham, MA) 5800 pulser/receiver and Panametrics V301 1” diameter, focused (focal length = 1.5”), broadband transducers with center frequencies of 500 kHz. Bone samples were placed in the focal

plane. The diameter of the central lobe of the focused beam at the focal plane ranged from 18 mm to 8 mm across the analysis band from 300 kHz to 700 kHz. (The central lobe width is given by $2.44\lambda z/d$, where λ = wavelength, z = focal length, and d = transducer aperture diameter (Goodman, 1968)). The central portions of the samples were scanned in order to approximate as closely as possible the ROI used in the DXA measurements. Received signals were digitized (8 bit, 10 MHz) using a LeCroy (Chestnut Ridge, NY) 9310C Dual 400 MHz oscilloscope and stored on computer (via GPIB) for off-line analysis.

A through-transmission method was used to measure normalized broadband ultrasonic attenuation (nBUA) and velocities. Using two opposing coaxially-aligned transducers (one transmitter and one receiver), transmitted signals were recorded both with and without the bone sample in the acoustic path. The bone samples were larger in cross-sectional area than the receiving transducer aperture. Attenuation coefficient was estimated using a log spectral difference technique (Kuc and Schwartz, 1979). Attenuation was characterized by the slope of a least-squares linear fit of attenuation coefficient (dB/cm) vs. frequency, resulting in the nBUA (dB/cmMHz) (Langton 1996). Phase velocity and signal velocity were measured using methods published previously (Wear, 2000a; Wear, 2000b; Wear, 2007. For signal velocity, the third zero crossing in advance of pulse envelope maximum (which corresponded approximately to the leading edge of the pulse used in this investigation) was used as a time-of-arrival marker. Since the speed of sound in calcaneus, approximately 1475–1650 m/s (Droin *et al.*, 1998), is comparable to that in distilled water at room temperature, approximately 1480–1490 m/s, potential diffraction-related errors (Xu and Kaufman 1993) in this substitution technique may be ignored (Droin *et al.* 1998). All frequency domain analysis was performed over the range from 300 kHz to 700 kHz.

Backscatter coefficients were measured using a reference phantom method (Yao *et al.*, 1990). Good agreement between experimental measurements using this method and theoretical predictions based on Faran's theory of scattering (Faran, 1951) for ultrasonic backscatter coefficients from phantoms consisting of glass spheres embedded in gelatin has previously been reported by this laboratory (Wear, 1999). The backscatter coefficient vs. frequency data were least-squares fit to a power law relationship over the range from 300 kHz to 700 kHz. The midband (500 kHz) value of the power law fit was used in the regression analysis. Backscatter data were gated to exclude the specular reflection at the front surface of the bone sample. Although backscatter measurements are less commonly used to characterize bone than attenuation and sound speed, many studies suggest that backscatter is a useful index of cancellous bone properties (Roberjot *et al.*, 1996; Wear and Garra, 1998; Wear, 1999; Hoffmeister *et al.*, 2000; Roux *et al*, 2001; Hoffmeister *et al.*, 2002; Jenson *et al.*, 2003; Wear and Laib, 2003; Hakulinen *et al.*, 2005; Hakulinen *et al.*, 2006; Jenson *et al.*, 2006; Hoffmeister *et al.*, 2006; Padilla *et al.*, 2006; Riekkinen *et al.*, 2007; Riekkinen *et al.*, 2008; Ta *et al.*, 2008; Padilla *et al.*, 2008; Wear, 2008; Karjalainen *et al.*, 2009; Litniewski *et al.*, 2009; Litniewski *et al.*, 2011; Hoffmeister, 2011; Padilla and Wear, 2011).

For both through-transmission and pulse-echo measurements, each bone sample was scanned (in 5 mm steps) along the major axis of the bone sample (see Figure 1) so that measurements were acquired from the purely cancellous portion of the bone (that is,

avoiding the cortical layer along the periphery). Thus, a frequency-dependent volume of interest was swept out with dimensions approximately [1.8 cm (at 300 kHz) – 0.8 cm (at 700 kHz)] × 3.6 cm × 1.8 cm (where the last dimension corresponds to the bone sample thickness, which is in the direction perpendicular to the plane of Figure 1). Since backscatter data were gated to exclude specular reflections at the front surfaces of calcaneus samples, backscatter volumes of interest were a few millimeters smaller in the thickness dimension than attenuation and velocity volumes of interest. Since an ultrasound beam has maximum intensity near its axis of symmetry, the ultrasound measurements were influenced more by the properties of the central regions of the bone samples than the noncentral regions. This is in contrast to the DXA and microCT measurements, which measured the bone samples essentially uniformly throughout the volumes of interest. This disparity in measurement spatial uniformity could reduce correlations between ultrasound and x-ray-based measurements, especially for highly inhomogeneous bone samples.

E. Data Analysis

Stepwise multiple regression analysis was performed to build linear models of ultrasound parameters as functions of BMD and microarchitectural features. The MATLAB (Natick, MA) function “stepwise” was used. In the case of backscatter coefficient, the data were log transformed prior to multiple regression analysis.

III. RESULTS

Figure 1 shows a slice of a microCT image of a calcaneus sample.

Table 1 shows the means, standard deviations, minima and maxima of ultrasound parameters, density, and microarchitectural parameters. The SMI, which in general can vary from 0 for plate-like architectures to 3 for rod-like architectures (Hildebrand and Ruegsegger, 1997) had a mean value of 2.34, suggesting that the bone samples tended to be more rod-like than plate-like.

Table 2 shows Pearson’s correlation coefficients between BMD and microarchitectural parameters. Table 3 shows Pearson’s correlation coefficients between ultrasound parameters and BMD / microarchitectural parameters. The best univariate predictors of the ultrasound parameters were the indexes of bone quantity, BV/TV and BMD.

Figure 2 shows measurements of nBUA plotted vs. BV/TV for the 29 bone samples. A linear regression fit to the data, BUA (dB/cmMHz) = −0.31 + 125.5 × BV/TV, is also shown.

Figure 3 shows measurements of phase velocity at 500 kHz (PV) plotted vs. BV/TV for the 29 bone samples. The dotted line shows the linear fit to data from parallel-nylon-wire phantoms previously reported (Wear, 2005), suggesting that empirical dependence of phase velocity on BV/TV is similar in cancellous bone samples and parallel-nylon-wire phantoms. (Aluminum-foam phantoms also exhibit ultrasonic properties similar to cancellous bone (Le *et al.*, 2010; Zhang *et al.*, 2011)). Figure 3 also shows theoretical predictions of the dependence of phase velocity on BV/TV predicted using Biot and Biot-related theory for poroelastic solids.

Figure 4 shows measurements of backscatter coefficient plotted vs. BV/TV for the 29 bone samples. A power law fit to the data is also shown.

Table 4 shows univariate and multivariate regression models that predict ultrasound parameters from BMD and microarchitectural parameters. Multiple regressions resulted in substantial increases (over univariate regressions based on BMD) in the adjusted squared correlation coefficients for nBUA and backscatter coefficient, and a moderate increase for phase velocity.

IV. DISCUSSION

Regarding the statistical aspects of the dependencies of nBUA, phase velocity, and backscatter coefficient on BMD and microarchitecture in human calcaneus, the regression analysis presented in this paper is for the most part in agreement with two previous reports (Nicholson *et al.*, 2001; Chaffai *et al.*, 2002). As with previous investigations with nBUA and phase velocity (Nicholson *et al.*, 2001) or nBUA, phase velocity and backscatter coefficient (Chaffai *et al.*, 2002), the best univariate predictors of the ultrasound parameters were the indexes of bone quantity, BMD and BV/TV. The best univariate models for nBUA, phase velocity, and backscatter coefficient yielded squared correlation coefficients of 0.69 – 0.73, a little lower on average than values reported by Nicholson *et al.* (2001), 0.74, and Chaffai *et al.* (2002), 0.71 – 0.81. Multiple regression models for attenuation, phase velocity and backscatter raised squared adjusted correlation coefficients to 0.74 – 0.83, consistent with values reported by Nicholson *et al.* (2001), 0.82, and Chaffai *et al.* (2002), 0.79 – 0.81.

Table 5 shows univariate correlation coefficients between ultrasound parameters and indexes of bone quantity in human calcaneus *in vitro* for the present study and previous studies by Nicholson *et al.* (2001) and Chaffai *et al.* (2002). The studies show moderate agreement. The correlation coefficients from Chaffai *et al.* (2002) tended to be higher than those for the present study, especially for phase velocity vs. BV/TV, backscatter coefficient vs. BV/TV, and backscatter coefficient vs. BMD. However, as shown in Table 5, the correlation coefficients from Chaffai *et al.* (2002) in all cases were within or near (±0.01) the high end of the 95% confidence intervals for the correlation coefficients from the present study. Moreover, it is possible that the widths of the 95% confidence intervals for correlation coefficients for Chaffai *et al.* were comparable to those for the present study since the numbers of samples for the two studies were similar (25 vs. 29). If so, this would imply overlap in 95% confidence intervals for the two studies. However, if differences in correlation coefficients between the two studies are meaningful, then there are some potential contributing factors that might help explain this. First, there may have been biological differences in the populations studied, as evidenced by the differences in Tb.Th: 72 ± 18 μm (Chaffai *et al.*) vs. 127 ± 17 μm (present study). Second, Chaffai *et al.* used sample volumes that were thinner in the ultrasound propagation direction (approximately 1 cm vs. approximately 1.8 cm for attenuation and velocity—slightly smaller in both studies for backscatter since gating was performed to exclude specular echoes) perhaps resulting in greater intra-sample homogeneity. Third, Chaffai *et al.* performed microCT analysis on 7-mm-diameter-cylindrical cores rather than 1.6 cm × 3.6 cm × 1.6 cm rectangular-shaped volumes the present study. Such small diameter samples may have been required for the

European Synchrotron Radiation Facility (ESRF) utilized by Chaffai *et al.*, which had a higher spatial resolution of 10 μm than the spatial resolution of 17.2 μm in the present study). Fourth, Chaffai *et al.* used a different frequency band of analysis (200 kHz – 600 kHz) than the one used in the present study (300 kHz – 700 kHz).

In the present study, the square of the correlation coefficient between signal velocity and BMD ($r^2 = 0.81$) was higher than the correlation between phase velocity and BMD ($r^2 = 0.74$) (see Table 5). Haïat *et al.*, (2005) reported similar results for human femur ($r^2 = 0.82$ for signal velocity and $r^2 = 0.67$ for phase velocity).

The statistical aspects of the dependencies of nBUA, phase velocity, and backscatter coefficient on BMD and microarchitecture in human calcaneus measured in this paper may be compared with results by others not only in human calcaneus but also in tibia and femur as shown in Table 6 and Figure 5 (Nicholson *et al.*, 1998;Trebacz and Natali, 1999;Nicholson *et al.*, 2001;Chaffai *et al.*, 2002;Hakulinen *et al.*, 2006;Padilla *et al.*, 2008;Karjalainen *et al.*, 2009). The average correlation coefficients for all three ultrasound parameters are relatively high, near 0.8, for the indexes of bone quantity (BMD and BV/TV) and lower for the remaining parameters. However, the relatively large ranges of values reported in different studies suggest that considerable uncertainty remains regarding the correlation coefficients between ultrasound parameters and microarchitectural features. Variances among different studies are probably due to a combination of differences in skeletal sites, sample preparation, ultrasound measurement methodology, microCT hardware and microarchitectural feature estimation algorithm. A recent report addresses the effect of microCT image resolution (Isaksson *et al.*, 2011).

CONCLUSION

Ultrasound parameters (attenuation, phase velocity, and backscatter), bone mineral density (BMD), and microarchitectural features were measured on 29 human cancellous calcaneus samples *in vitro*. Regression analysis was performed to predict ultrasound parameters from BMD and microarchitectural features. The best univariate predictors of the ultrasound parameters were the indexes of bone quantity: BMD and bone volume fraction (BV/TV). Therefore, attenuation, phase velocity, and backscatter coefficient are primarily determined by bone quantity, but multiple regression models based on bone quantity plus microarchitectural features achieve slightly better predictive performance than models based on bone quantity alone.

ACKNOWLEDGEMENTS

The authors are grateful to 1) the FDA Office of Women's Health for funding, 2) Dr. James Reynolds and Angela Stuber, NIH Clinical Center, who helped with DXA measurements, and 3) Dr. Andres Laib, Scanco Medical AG, Bruttisellen, Switzerland for producing a microCT image. The mention of commercial products, their sources, or their use in connection with material reported herein is not to be construed as either an actual or implied endorsement of such products by the Department of Health and Human Services. Certain equipment, instruments or materials are identified in this paper to adequately specify the experimental details. Such identification does not imply recommendation by the National Institute of Standards and Technology, nor does it imply the materials are necessarily the best available for the purpose.

Reference List

Alves JM, Ryaby JT, Kaufman JJ, Magee FP, and Siffert RS, 1996, "Influence of marrow on ultrasonic velocity and attenuation in bovine trabecular bone," Calcif. Tissue Int. 58, 362–367. [PubMed: 8661972]

Aygun H, Attenborough K, Postema M, Lauriks W, and Langton CM, (2009), "Predictions of angle dependent tortuosity and elasticity effects on sound propagation in cancellous bone," J. Acoust. Soc. Am, 126, 3286–3290. [PubMed: 20000942]

Barkmann R, and Glüer C-C, 2011, "Clinical Applications" in Bone Quantitative Ultrasound, ed. Laugier P and Haiat G, Springer, New York, NY, chapter 4, 73–82.

Biot MA (1956a), "Theory of propagation of elastic waves in a fluid saturated porous solid I. Low frequency range," J. Acoust. Soc. Am 28, 168–178.

Biot MA (1956b), "Theory of propagation of elastic waves in a fluid saturated porous solid II. High frequency range," J. Acoust. Soc. Am 28, 179–191.

Biot MA (1956c), "Theory of deformation of a porous viscoelastic anisotropic solid." J. Appl. Phys, 27, 459–467.

Biot MA (1962), "Generalized theory of acoustic propagation in porous dissipative media," J. Acoust. Soc. A, 34, 1254–1264.

Biot MA (1963), "Mechanics of deformation and acoustic propagation inporous media," J. Appl. Phys, 33, 1482–1498.

Buchanan JL, Gilbert RP, and Ou M, (2011). "Transfer functions for a one-=dimensional fluid-poroelastic system subject to an ultrasonic pulse," Nonlinear Analysis: Real World Applications, in press.

Cardoso L, Teboul F, Sedel L, Oddou C, and Meunier A, (2003). "In vitro acoustic waves propagation in human and bovine cancellous bone," J. Bone. Miner. Res, 18, 1803–1812. [PubMed: 14584891]

Cardoso L, Meunier A, and Oddou C, (2008). "In vitro acoustic wave propagation in human and bovine cancellous bone as predicted by Biot's theory," J. Mech. Med., Biol, 8, 183–201.

Cardoso L, Cowin SC, (2011). "Fabric dependence of quasi-waves in anisotropic porous media," J. Acoust. Soc. Am, 129, 3302–3316. [PubMed: 21568431]

Cowin SC, and Cardoso L, (2010). "Fabric dependence of wave propoagation in anisotropic porous media," Biomech. Model Mechanobiol, Published online 12 May 2010. .

Chaffai S, Roberjot V, Peyrin F, Berger G, and Laugier P, 2000, "Frequency dependence of ultrasonic backscatter in cancellous bone: autocorrelation model and experimental results," J. Acoust., Soc. Am, 108, 2403–2411. [PubMed: 11108380]

Chaffai S, Peyrin F, Nuzzo S, Porcher R, Berger G, and Laugier P, 2002, "Ultrasonic characterization of human cancellous bone using transmission and backscatter measurements: relationships to density and microstructure," Bone 30, 229–237. [PubMed: 11792590]

Droin P, Berger G, and Laugier P, 1998, "Velocity dispersion of acoustic waves in cancellous bone," IEEE Trans. Ultrason. Ferroelectr. Freq. Control 45, 581–592. [PubMed: 18244210]

Faran JJ, 1951, "Sound scattering by solid cylinders and spheres," J Acoust. Soc. Am 23, 405–418.

Fellah ZEA, Chapelon JY, Berger S, Lauriks W, and Depollier C, (2004). "Ultrasonic wave propagation in human cancellous bone: application of Biot theory, J. Acoust. Soc. Am, 116, 61–73. [PubMed: 15295965]

Fellah ZEA, Sebaa N, Fellah M, Mitri FG, Ogam E, Lauriks W, and Depollier C, (2008). "Application of the Biot model to ultrasound in bone: direct problem," IEEE Trans Ultrason, Ferro, and Freq Cont, 55, 1508–1515.

Goodman JW, Introduction to Fourier Optics, McGraw-Hill, San Francisco, CA, 1968, p.64

Haïat G, Padilla F, Barkmann R, Dencks S, Moser U, Glüer CC, and Laugier P (2005), "Optimal prediction of bone mineral density with ultrasonic measurements in excised human femur," Calcif. Tissue Int, 77, 186–192. [PubMed: 16151672]

Haïat G, Lhemery A, Renaud F, Padilla F, Laugier P, and Naili S, 2008, "Velocity dispersion in trabecular bone: influence of multiple scattering and of absorption," J Acoust. Soc. Am 124, 4047–4058. [PubMed: 19206827]

Haire TJ, and Langton CM (1999), "Biot Theory: A review of its application to ultrasound propagation through cancellous bone," Bone, 24, 291–295. [PubMed: 10221540]

Hakulinen MA, Day JS, Toyras J, Timonen M, Kroger H, Weinans H, Kiviranta I, and Jurvelin JS, (2005), "Prediction of density and mechanical preoperties of human trabecular bone in vitro by using ultrasound transmission and backscattering measurements at 0.2–6.7 MHz frequency range," Phys. Med., Biol, 50, 1629–1642. [PubMed: 15815086]

Hakulinen MA, Day JS, Toyras J, Weinans H, and Jurvelin JS, 2006, "Ultrasonic characterization of human trabecular bone microstructure," Phys. Med Biol. 51, 1633–1648. [PubMed: 16510968]

Hildebrand T, Laib A, Muller R, Dequeker J, and Ruegsegger P, 1999, "Direct three-dimensional morphometric analysis of human cancellous bone: microstructural data from spine, femur, iliac crest, and calcaneus," J Bone Miner. Res 14, 1167–1174. [PubMed: 10404017]

Hildebrand T and Ruegsegger P, 1997, "Quantification of Bone Microarchitecture with the Structure Model Index," Comput. Methods Biomech. Biomed. Engin 1, 15–23. [PubMed: 11264794]

Hoffmeister BK, Whitten SA, Rho JA, 2000, "Low-Megahertz ultrasonic properties of bovine cancellous bone," Bone, 26, 635–642. [PubMed: 10831936]

Hoffmeister BK, Auwarter JA, and Rho JY, 2002, "Effect of marrow on the high frequency ultrasonic properties of cancellous bone," Phys. Med Biol. 47, 3419–3427. [PubMed: 12375829]

Hoffmeister BK, Jones CI, Caldwell GJ, and Kaste SC, 2006, "Ultrasonic characterizatin of cancelllous bone using apparent integrated backscatter," Phys., Med., Biol, 51, 2715–2727. [PubMed: 16723761]

Hoffmeister BK, (2011), "Frequency dependence of apparent ultrasonic backscatter from human cancellous bone," Phys., Med., Biol, 56, 667–683. [PubMed: 21220842]

Hosokawa A, and Otani T, (1997). "Ultrasonic wave propagation in bovine cancellous bone," J. Acoust. Soc. Am, 101, 558–562. [PubMed: 9000743]

Hosokawa A and Otani T 1998, "Acoustic anisotropy in bovine cancellous bone," J. Acoust. Soc. Am, 103, 2718–2722. [PubMed: 9604363]

Hosokawa A (2005). "Simulation of ultrasound propagation through bovine cancellous bone using elastic and Biot's finite-difference time-domain methods," J Acoust Soc Am, 118, 1782–1789. [PubMed: 16240836]

Hosokawa A, (2008) "Development of a numerical cancellous bone model for finite-difference time-domain simulations of ultrasound propagation," IEEE Trans Ultrason, Ferro, Freq Cont, 55, 1219–1233.

Hughes ER, Leighton TG, Petley GW, White PR, and Chivers RC, (2003), "Estimation of critical and viscous frequencies for Biot theory in cancellous bone," Ultrasonics, 41, 365–368. [PubMed: 12788218]

Hughes ER, Leighton TG, White PR, and Petley GW, (2007) "Investigation of an anisotropic tortuosity in a Biot model of ultrasonic propagation in cancellous bone," J. Acoust. Soc. Am, 121, 568–574. [PubMed: 17297810]

Isaksson H, Toyras J, Hakulinen M, Aula AS, Tamminen I, Julkunen P, Kroger H, and Jurvelin JS, 2011, "Structural parameters of normal and osteoporotic human trabecular bone are affected differently by microCT image resolution," Osteoporos. Int, 22, 167–177. [PubMed: 20349043]

Jenson F, Padilla F, and Laugier P, (2003). "Prediction of frequency-dependent ultrasonic backscatter in cancellous bone using statistical weak scattering model." Ultrasound in Med., & Biol, 29, 455–464. [PubMed: 12706197]

Jenson F, Padilla F, Bousson V, Bergot C, Laredo J-D, and Laugier P, (2006). "In vitro ultrasonic characterization of human cancellous femoral bone using transmission and backscatter measurements: relationships to bone mineral density," J. Acoust. Soc. Am, 119, 654–663. [PubMed: 16454319]

Karjalainen JP, Toyras J, Riekkinen O, Hakulinen M, and Jurvelin JS, 2009, "Ultrasound backscatter imaging provides frequency-dependent information on structure, composition and mechanical properties of human trabecular bone," Ultrasound Med Biol. 35, 1376–1384. [PubMed: 19525060]

Krieg MA, Barkmann R, Gonnelli S, Stewart A, Bauer DC, Barquero LDR, Kaufman JJ, Lorenc R, Miller PD, Olszynski WP, Poiana C, Schott AM, Lewiecki EM, and Hans D, 2008, "Quantitative

ultrasound in the management of osteoporosis: the 2007 ISCD Official Positions," J Clin Densitom. 11, 163–187. [PubMed: 18442758]

Kuc R and Schwartz M, 1979, "Estimating the acoustic attenuation coefficient slope for liver from reflected ultrasound signals," IEEE Trans. Sonics Ultrason. SU-26, 353–362.

Langton CM, Njeh CF, Hodgskinson R, and Currey JD, 1996, "Prediction of mechanical properties of the human calcaneus by broadband ultrasonic attenuation," Bone 18, 495–503. [PubMed: 8805988]

Langton CM, Palmer SB, and Porter RW, 1984, "The measurement of broadband ultrasonic attenuation in cancellous bone," Eng. Med 13, 89–91. [PubMed: 6540216]

Laugier P, 2008, "Instrumentation for in vivo ultrasonic characterization of bone strength," IEEE Trans. Ultrason. Ferroelectr. Freq. Control 55, 1179–1196. [PubMed: 18599407]

Laugier P, 2011, "Quantitative Ultrasound Instrumentation for Bone In Vivo Characterization" in Bone Quantitative Ultrasound, ed. Laugier P and Haiat G, Springer, New York, NY, chapter 3, 47–72.

Le LH, Zhang C, Ta D, Lou E, (2010), "Measurement of tortuosity in aluminum foams using airborne ultrasound," Ultrasonics, 50, 1–5. [PubMed: 19720388]

Lee KI, Roh H, and Yoon SW (2003), "Acoustic wave propagation in bovine cancellous bone: Application of the modified Biot-Attenborough model," J. Acoust. Soc. Am, 114, 2284–2293. [PubMed: 14587625]

Lee KI, and Yoon SW (2006). "Comparison of acoustic characteristics predicted by Biot's theory and the modified Biot-Attenborough model in cancellous bone, J Biomech, 39, 364–368. [PubMed: 16321640]

Litniewski J, Nowicki A, and Lewin P, (2009). "Semi-empirical bone model for determination of trabecular structure properties from backscatter ultrasound." Ultrasonics, 49, 505–513. [PubMed: 19232659]

Litniewski J, Cieslik L, Wojcik J, and Nowicki A (2011). "Statistics of the envelope of ultrasonic backscatter from human trabecular bone," J. Acoust. Soc. Am, 130, 2224–2232. [PubMed: 21973377]

McKelvie ML, and Palmer SB (1991), "The interaction of ultrasound with cancellous bone," Phys. Med. Biol, 36, 1331–1340. [PubMed: 1745661]

Mohamed MM, Shaat LT, and Mahmoud AN, (2003), "Propagation of ultrasonic waves through demineralized cancellous bone," IEEE Trans. Ultrason., Ferro., and Freq. Cont, 50, 279–288.

Nicholson PH and Bouxsein ML, 2002, "Bone marrow influences quantitative ultrasound measurements in human cancellous bone," Ultrasound Med Biol. 28, 369–375. [PubMed: 11978417]

Nicholson PH, Muller R, Cheng XG, Ruegsegger P, Van Der PG, Dequeker J, and Boonen S, 2001, "Quantitative ultrasound and trabecular architecture in the human calcaneus," J Bone Miner. Res 16, 1886–1892. [PubMed: 11585354]

Nicholson PH, Muller R, Lowet G, Cheng XG, Hildebrand T, Ruegsegger P, Van Der PG, Dequeker J, and Boonen S, 1998, "Do quantitative ultrasound measurements reflect structure independently of density in human vertebral cancellous bone?," Bone 23, 425–431. [PubMed: 9823448]

Njeh CF and Langton CM, 1997, "The effect of cortical endplates on ultrasound velocity through the calcaneus: an in vitro study," Br. J Radiol. 70, 504–510. [PubMed: 9227233]

Padilla F, Jenson F, and Laugier P, 2006, "Estimation of trabecular thickness using ultrasonic backscatter," Ultrasonic Imaging, 28, 3–22. [PubMed: 16924879]

Padilla F, Jenson F, Bousson V, Peyrin F, and Laugier P, 2008, "Relationships of trabecular bone structure with quantitative ultrasound parameters: in vitro study on human proximal femur using transmission and backscatter measurements," Bone 42, 1193–1202. [PubMed: 18396124]

Padilla F, and Wear K, 2011, "Scattering by Trabecular Bone" in Bone Quantitative Ultrasound, ed. Laugier P and Haiat G, Springer, New York, NY., chapter 6, 123–146.

Pakula M, and Kubik J, (2002). "Propagation of ultrasonic waves in cancellous bone. Micro and macrocontinual approach," Poromechanics II, ed. By Auriault JL, Geindreau C, Royer P, Block J-F, Boutin C, and Lewandowska L Swets and Zeitlinger, Lisse, 65–70.

Pakula M, Padilla F, Laugier P, Kaczmarek M, 2008, "Application of Biot's theory to ultrasonic characterization of human cancellous bones: Determination of structural, material, and mechanical properties," J. Acoust. Soc. Am, 123, 2415–2423. [PubMed: 18397044]

Riekkinen O, Hakulinen MA, Lammi MJ, Jurvelin JS, Kallioniemi A, and Toyras J, (2007), "Acoustic properties of trabecular bone--relationships to tissue composition," Ultrasound in Med., & Biol, 33, 1438–1444. [PubMed: 17561333]

Riekkinen O, Hakulinen MA, Toyras J, and Jurvelin JS (2008), "Dual-frequency ultrasound--new pulse-echo technique for bone densitometry," Ultrasound in Med., & Biol, 34, 1703–1708. [PubMed: 18524463]

Roberjot V, Laugier P, Droin P, Giat P, and Berger G, 1996, "Measurement of integrated backscatter coefficient of trabecular bone," 1996 IEEE Ultrasonics Symp. Proc., cat., no. 96CH35993, vol. 2, 1123–6.

Roux C, Roberjot V, Porcher R, Kolta S, Dougados M, and Laugier P (2001). "Ultrasonic backscatter and transmission parameters at the os calcis in postmenopausal osteoporosis," J., Bone & Mineral Res, 16, 1353–1362.

Ruegsegger P, Koller B, and Muller R, 1996, "A microtomographic system for the nondestructive evaluation of bone architecture," Calcif. Tissue Int. 58, 24–29. [PubMed: 8825235]

Sebaa N, Fellah ZEA, Fellah M, Ogam E, Mitri FG, Depollier C, and Lauriks W (2008). "Application of the Biot model to ultrasound in bone: inverse problem," IEEE Trans Ultrason, Ferro, and Freq Cont, 55, 1516–1523.

Ta D, Wang W, Huang K, and Wang Y, 2008, "Analysis of frequency dependence of ultrasonic backscatter coefficient in cancellous bone," J. Acoust. Soc. Am, 124(6), 4083–4090. [PubMed: 19206830]

Trebacz H and Natali A, 1999, "Ultrasound velocity and attenuation in cancellous bone samples from lumbar vertebra and calcaneus," Osteoporos. Int 9, 99–105. [PubMed: 10367035]

Ulrich D, van Rietbergen B, Laib A, and Ruegsegger P, 1999, "The ability of three-dimensional structural indices to reflect mechanical aspects of trabecular bone," Bone 25, 55–60. [PubMed: 10423022]

Wear KA, and Garra B,S, 1998, "Assessment of bone density using ultrasonic backscatter," Ultrasound Med., Biol, 24, 689–695. [PubMed: 9695272]

Wear KA, 1999, "Frequency dependence of ultrasonic backscatter from human trabecular bone: theory and experiment," J Acoust. Soc. Am 106, 3659–3664. [PubMed: 10615704]

Wear KA, 2000a, "Measurements of phase velocity and group velocity in human calcaneus," Ultrasound Med Biol. 26, 641–646. [PubMed: 10856627]

Wear KA, 2000b, "The effects of frequency-dependent attenuation and dispersion on sound speed measurements: applications in human trabecular bone," IEEE Trans. Ultrason. Ferroelectr. Freq. Control 47, 265–273. [PubMed: 18238539]

Wear KA, and Laib A, 2003, "The dependence of ultrasonic backscatter on trabecular thickness in human calcaneus: theoretical and experimental results," IEEE Trans Ultrason. Ferro., and Freq. Cont, 50, 979–986.

Wear KA, 2005, "The dependencies of phase velocity and dispersion on trabecular thickness and spacing in trabecular bone-mimicking phantoms," J Acoust. Soc. Am 118, 1186–1192. [PubMed: 16158673]

Wear KA, 2007, "The dependence of time-domain speed-of-sound measurements on center frequency, bandwidth, and transit-time marker in human calcaneus in vitro," J Acoust. Soc. Am 122, 636–644. [PubMed: 17614520]

Wear KA 2008, "Ultrasonic scattering from cancellous bone: a review," IEEE Trans. Ultrason., Ferro., and Freq. Cont, 55, 1432–1441.

Wear KA and Laib A, 2003, "The dependence of ultrasonic backscatter on trabecular thickness in human calcaneus: theoretical and experimental results," IEEE Trans. Ultrason. Ferroelectr. Freq. Control 50, 979–986. [PubMed: 12952089]

Wear KA, Laib A, Stuber AP, Reynolds JC, 2005, "Comparison of measurements of phase velocity in human calcaneus to Biot theory," J. Acoust. Soc. Am, 117, 3319–3324. [PubMed: 15957798]

Wear KA, Padilla F, and Laugier P, 2008, "Comparison of the Faran cylinder model and the weak scattering model for predicting the frequency dependence of backscdatter from human cancellous femur *in vitro*," J. Acoust. Soc. Am, 124, 1408–1410. [PubMed: 19045632]

Williams JL, 1992, "Ultrasonic wave propagation in cancellous and cortical bone: predictions of some experimental results by Biot's theory," J. Acoust. Soc. Am 92, 1106–1112.

Xia Y, Lin Wei, and Qin Y-X, (2005), "The influence of cortical end-plate on broadband ultrasound attenuation measurements at the human calcaneus using scanning confocal ultrasound," J. Acoust. Soc. Am, 118, 1801–1807. [PubMed: 16240838]

Xu W, and Kaufman JJ, 1993, "Diffraction correction methods for insertion ultrasound attenuation estimation," IEEE Trans. Biomed. Eng, 40, 563–569. [PubMed: 8262538]

Yao LX, Zagzebski JA, and Madsen EL, 1990, "Backscatter coefficient measurements using a reference phantom to extract depth-dependent instrumentation factors," Ultrason. Imaging 12, 58–70. [PubMed: 2184569]

Zhang C, Le LH, Zheng R, Ta D, and Lou E (2011). "Measurements of ultrasonic phase velocities and attenuation of slow waves in cellular aluminum foams as cancellous bone-mimicking phantoms," J. Acoust. Soc. Am, 129, 3317–3326. [PubMed: 21568432]

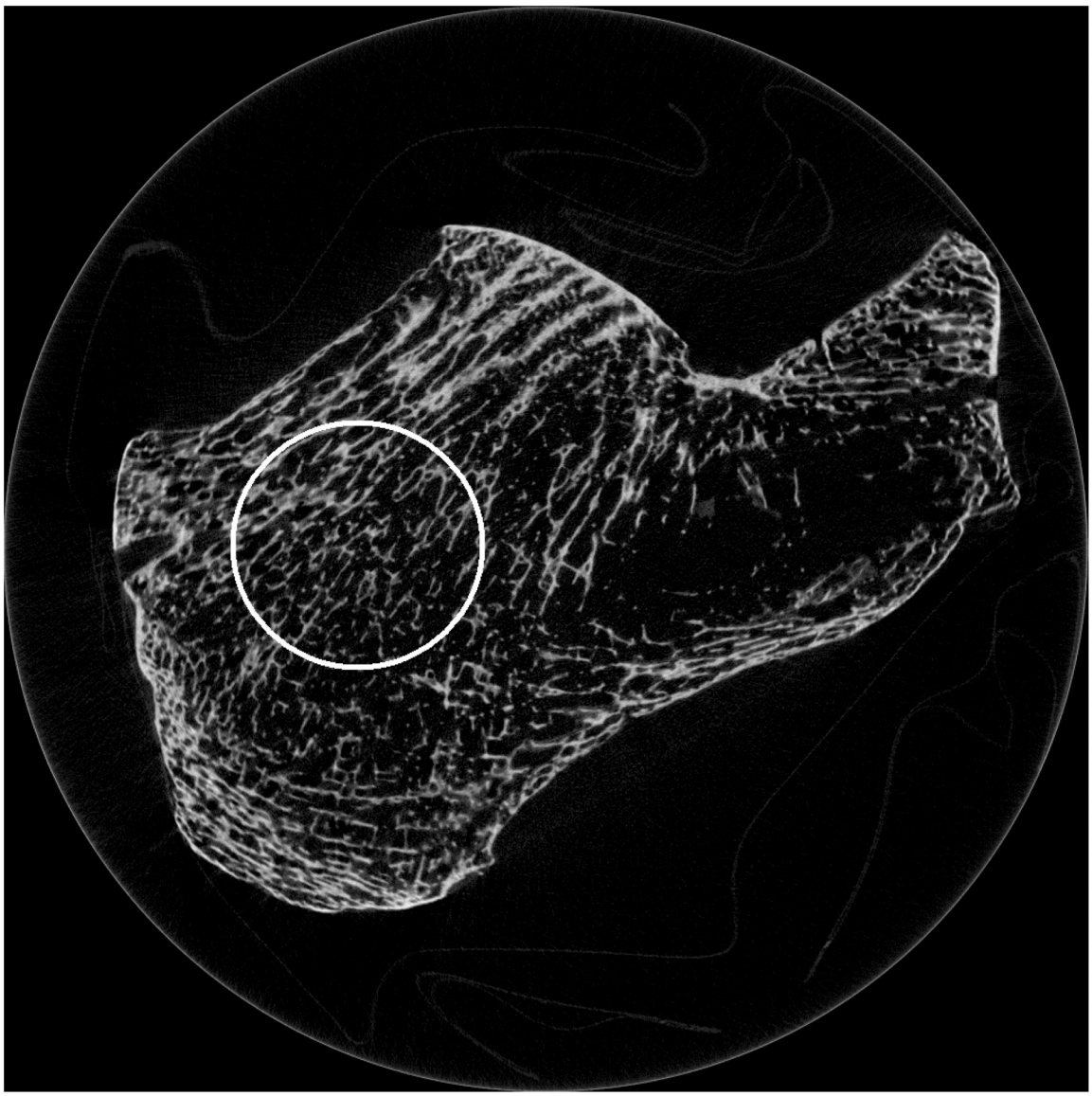

1.

A slice from a micro-computed tomogram of calcaneus. Some trabeculae appear to terminate as they move into and out of the imaging plane. Image acquired by Andres Laib, Scanco Medical AG, Bruttisellen, Switzerland. A −3 dB beam cross section at 500 kHz is shown.

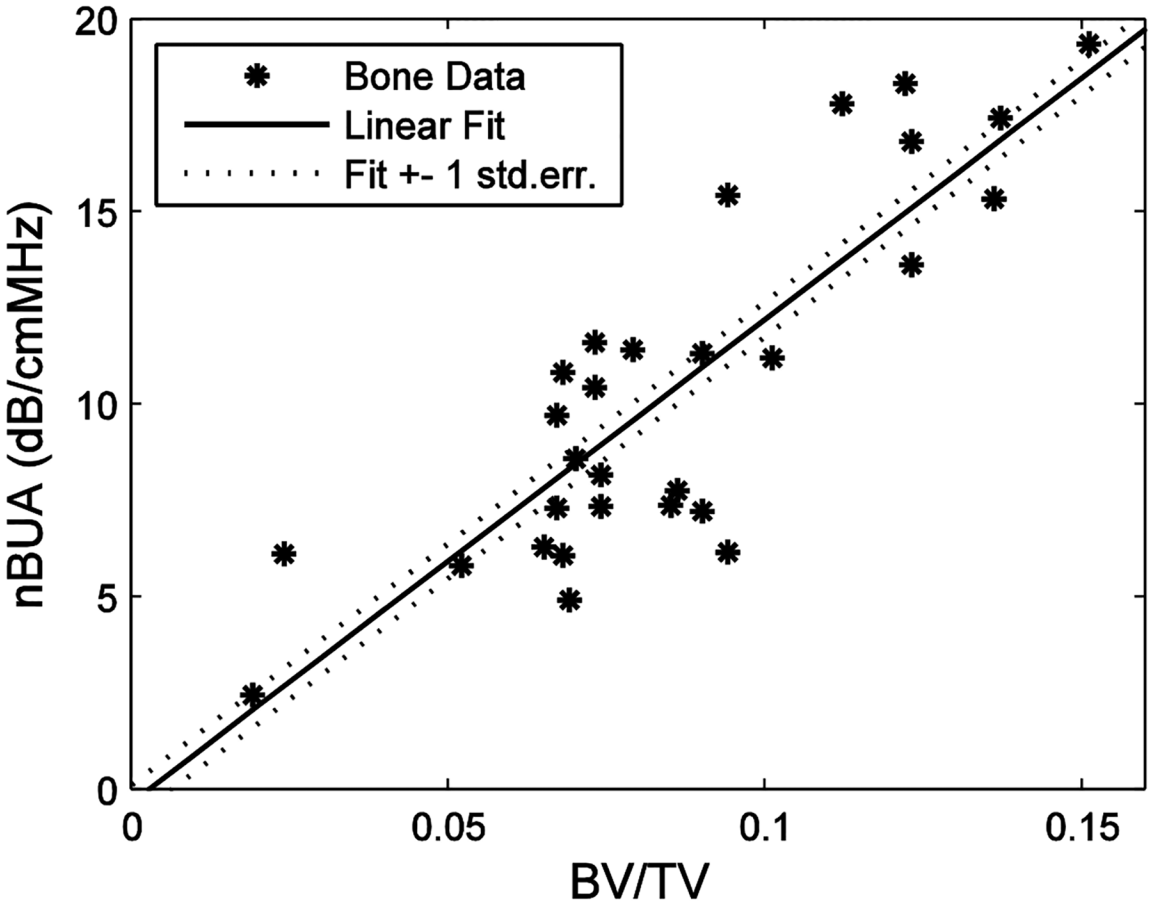

2.

Measurements of nBUA plotted vs. BV/TV for the 29 bone samples. A linear regression fit to the data is also shown. The dotted lines show the linear regression fit plus or minus one standard error.

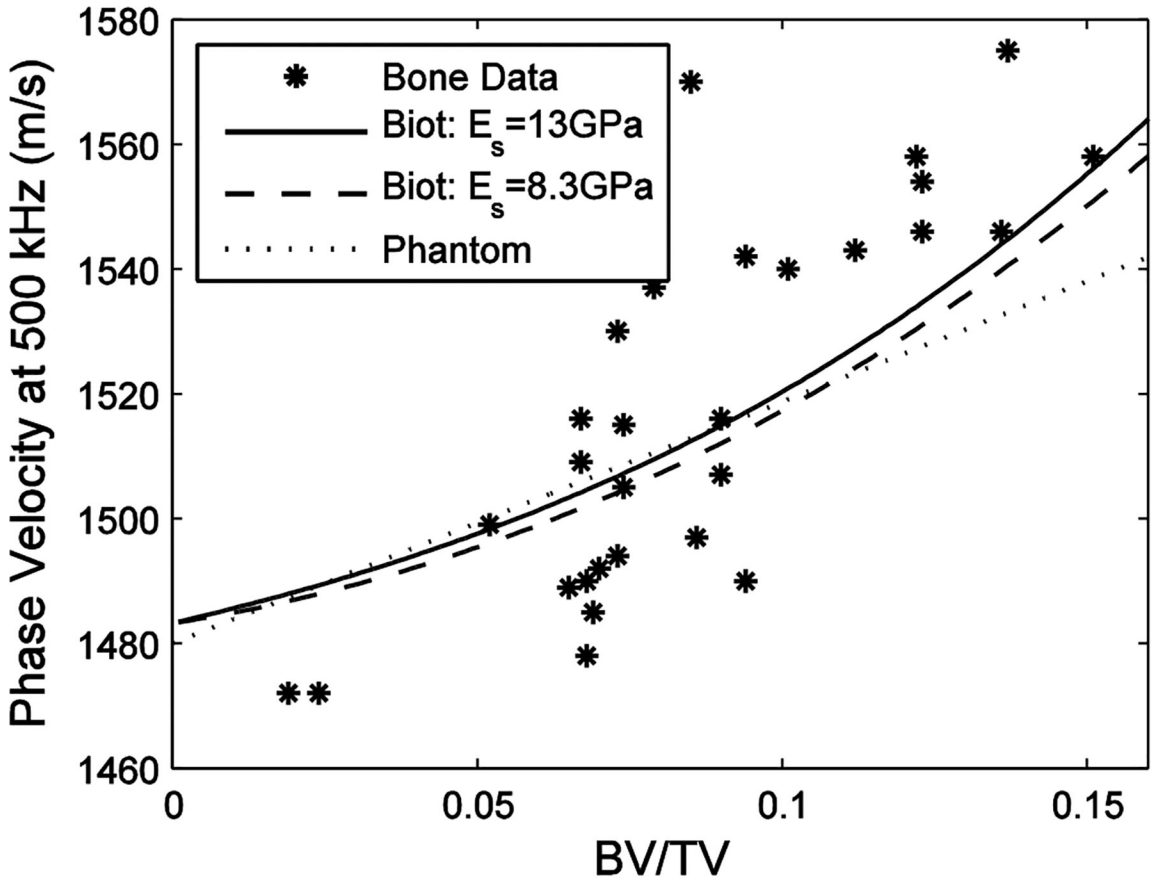

3.

Measurements of phase velocity (PV) (at 500 kHz) plotted vs. BV/TV for the 29 bone samples. The dotted line shows the linear fit to data from parallel-nylon-wire phantoms previously reported (Wear, 2005). The other lines show theoretical forms based on Biot theory (Biot 1956a, 1956b, 1956c, 1962, 1963), which has been applied to bone by many investigators (McKelvie and Palmer 1991; Williams 1992; Hosokawa and Otani 1997, 1998; Haire and Langton 1999; Pakula and Kubik, 2002; Hughes *et al.* 2003; Lee *et al.* 2003; Mohamed *et al.* 2003; Cardoso *et al.* 2003; Fellah *et al.* 2004; Hosokawa, 2005; Wear *et al.* 2005; Lee and Yoon 2006; Hughes *et al.* 2007; Pakula *et al.* 2008; Fellah *et al.* 2008; Sebaa *et al.* 2008; Cardoso *et al.*, 2008; Aygun *et al.*, 2009; Cowin and Cardoso, 2010; Buchanan *et al.*, 2011; Cardoso and Cowin, 2011). The parameters for theoretical predictions were fluid (water) density = 1 g/cm^3, fluid viscosity = 0.01 g /cm·s, bulk modulus of fluid = 2.2 GPa, density of solid phase = 1.8 g/cm^3, Young's modulus of the solid phase (E_s) = 13 GPa or 8.3GPa, Poisson's ratio of solid phase = 0.32, Poisson's ratio of trabecular frame = 0.23. The values for the exponent m, where the Young's modulus of the skeletal frame $E_b = E_s (BV/TV)^m$, were m = 2.14 (for E_s = 13 GPa) or m = 1.75 (for E_s = 8.3 GPa) (Wear *et al.*, 2005; Pakula *et al*, 2008).

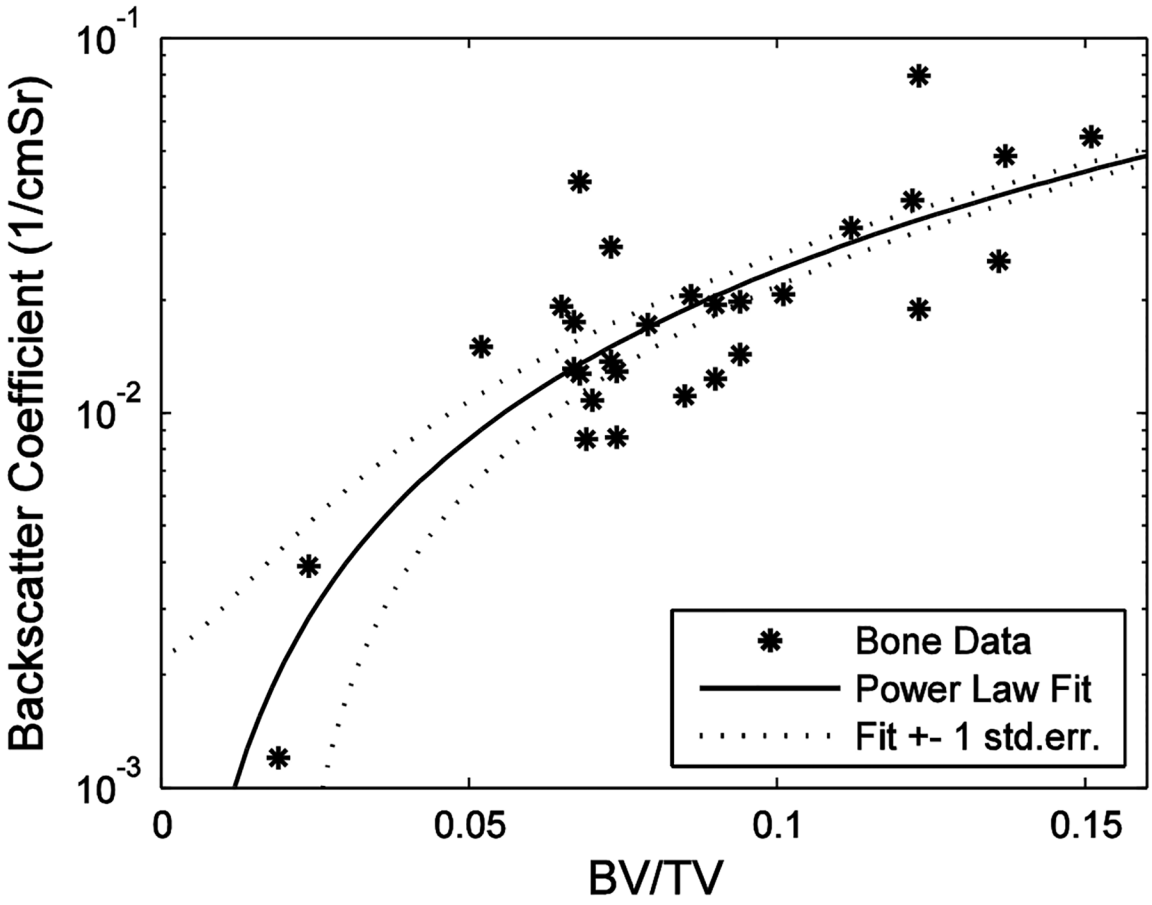

4.

Measurements of backscatter coefficient plotted vs. BV/TV for the 29 bone samples. A power law fit to the data is also shown. The dotted lines show the power law fit plus or minus one standard error.

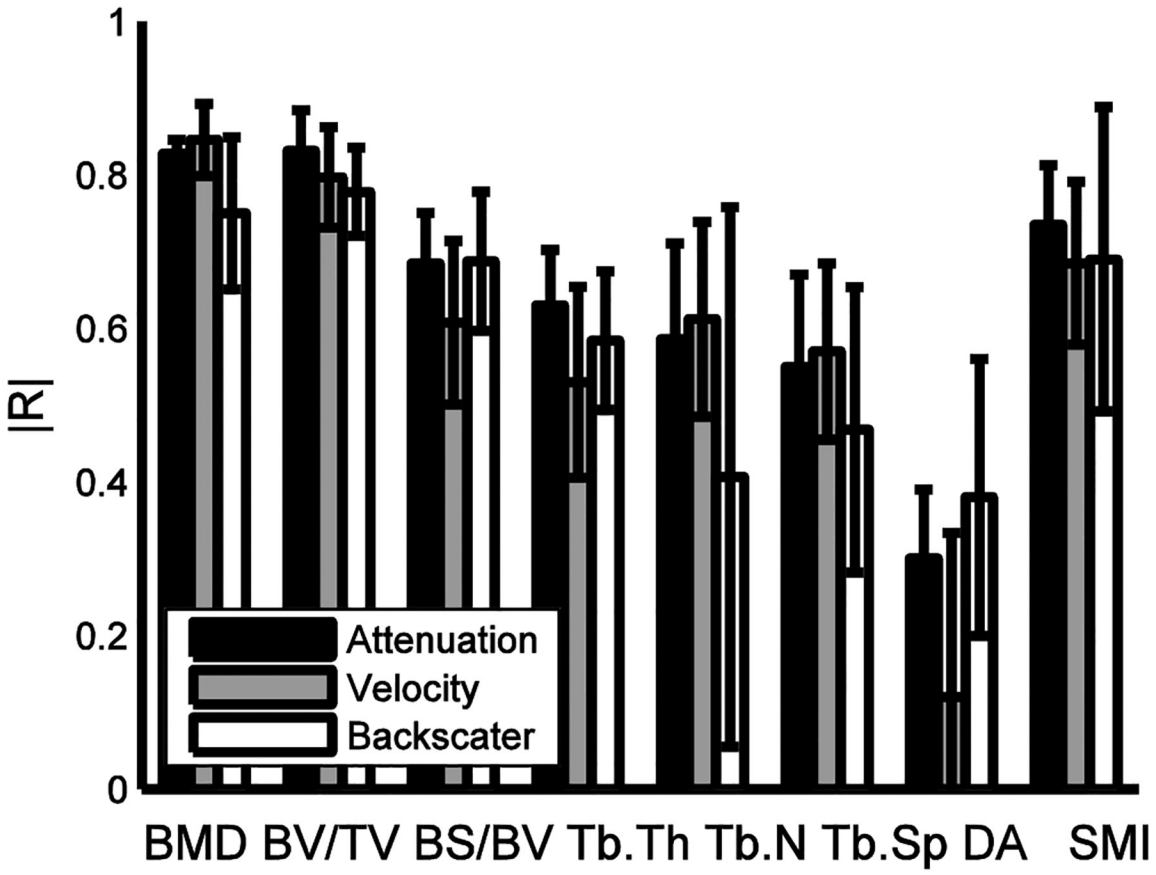

5.

Means for absolute values of correlation coefficients for ultrasound parameters versus BMD and microarchitectural features from the present study and seven others (Nicholson *et al.*, 1998;Trebacz and Natali, 1999;Nicholson *et al.*, 2001;Chaffai *et al.*, 2002;Hakulinen *et al.*, 2006;Padilla *et al.*, 2008;Karjalainen *et al.*, 2009). Error bars denote standard deviations.

Table 1.

Means, standard deviations, minima and maxima of ultrasound parameters density parameters and architectural parameters.

	Mean	Std.Dev.	Min	Max
Ultrasound parameters:				
nBUA (dB/cmMHz)	10.45	4.60	2.47	19.39
Signal velocity (m/s)	1543	40	1476	1615
Phase velocity (m/s)	1518	30	1472	1575
Backscat. Coef. (1/cmSr)	0.0219	0.0166	0.0012	0.0793
Density:				
BMD (g/cc)	0.122	0.056	0.002	0.201
Architectural parameters:				
BV/TV	0.086	0.031	0.019	0.151
BS/BV (1/mm)	22.0	3.1	16.2	30.2
Tb.Th (micron)	126	17	99	168
Tb.N (1/mm)	0.99	0.16	0.69	1.29
Tb.Sp (mm)	1.00	0.17	0.74	1.41
SMI	2.34	0.45	1.57	3.64
Connectivity (1/mm3)	3.74	1.26	1.50	6.99
DA	1.65	0.11	1.42	1.91
H1 (mm)	0.90	0.19	0.62	1.34
H2 (mm)	1.47	0.33	1.04	2.44
H3 (mm)	1.02	0.23	0.71	1.75

Table 2.

Pearson's correlation coefficients between BMD and architectural parameters. n: nonsignificant, a: $p < 0.05$, b: $p < 0.01$, c: $p < 0.001$, d: $p < 0.0001$.

	BMD	**BV/TV**	**BS/BV**	**Tb.Th**	**Tb.N**	**Tb.Sp**	**SMI**	**Conn**	**DA**	**H1**	**H2**	**H3**	
BMD	1.00d	0.78d	−0.56b	0.32n	0.12n	−0.19n	−0.74d	0.44a	0.29n	−0.71d	−0.57b	−0.64c	BMD
BV/TV		1.00d	−0.68d	0.49b	0.13n	−0.18n	−0.75d	0.41a	0.38a	−0.67d	−0.52b	−0.63c	BV/TV
BS/BV			1.00d	−0.91d	0.41a	−0.35n	0.73d	0.18n	−0.61c	0.17n	−0.04n	0.14n	BS/BV
Tb.Th				1.00d	−0.35n	0.30n	−0.46a	−0.32n	0.58c	0.00n	0.19n	−0.02n	Tb.Th
Tb.N					1.00d	−0.98d	0.24n	0.78d	−0.25n	−0.65c	−0.71d	−0.64c	Tb.N
Tb.Sp						1.00d	−0.22n	−0.75d	0.20n	0.69d	0.74d	0.65c	Tb.Sp
SMI							1.00d	−0.18n	−0.45a	0.48b	0.30n	0.43a	SMI
Conn								1.00d	−0.17n	−0.84d	−0.85d	−0.81d	Conn
DA									1.00d	−0.03n	0.29n	0.04n	DA
H1										1.00d	0.94d	0.89d	H1
H2											1.00d	0.87d	H2
H3												1.00d	H3

Table 3.

Pearson's correlation coefficients between ultrasound parameters and BMD and architectural parameters. n: nonsignificant, a: $p < 0.05$, b: $p < 0.01$, c: $p < 0.001$, d: $p < 0.0001$.

	BMD	BV/TV	BS/BV	Tb.Th	Tb.N	Tb.Sp	SMI	Conn	DA	H1	H2	H3
nBUA	0.80d	0.85d	−0.60c	0.50b	0.16n	−0.22n	−0.68d	0.37a	0.41a	−0.64c	−0.48b	−0.60c
Sig Velocity	0.90d	0.77d	−0.47a	0.30n	0.19n	−0.25n	−0.61c	0.43a	0.20n	−0.65c	−0.55b	−0.60c
PhaseVelocity	0.86d	0.81d	−0.45a	0.27n	0.21n	−0.26n	−0.63c	0.46a	0.23n	−0.65c	−0.54b	−0.61c
Backscat Coef	0.75d	0.84d	−0.75d	0.62c	−0.16n	0.14n	−0.83d	0.11n	0.60c	−0.47b	−0.27n	−0.38a

Table 4.

Linear regression models for ultrasound parameters. The third column is the square of the adjusted correlation coefficient of the regression. The fourth column is the increase in the square of the adjusted correlation coefficient compared to a univariate regression based on BMD as the independent variable.

Dependent Variable	Independent Variables	r_{adj}^2	Δr_{adj}^2
nBUA	BMD	0.63	
	BV/TV	0.70	
	BMD, BV/TV	0.75	0.12
	BMD, BV/TV, Tb.Th	0.76	0.13
	BMD, BV/TV, Tb.Th, BS/BV	0.82	0.19
	BMD, BV/TV, Tb.Th, BS/BV, Tb.N	0.83	0.20
Phase Velocity	BMD	0.73	
	BV/TV	0.64	
	BMD, BV/TV	0.77	0.04
	BMD, BV/TV, BS/BV	0.79	0.06
Signal Velocity	BMD	0.81	
	BV/TV	0.59	
	BMD, BV/TV, BS/BV, Tb.Th	0.84	0.03
Backscatter Coef.	BMD	0.54	
	BV/TV	0.69	
	BMD, BV/TV, Tb.Th	0.73	0.19
	BV/TV, Tb.Th	0.74	

Table 5.

Univariate correlation coefficients between ultrasound parameters and indexes of bone quantity in human calcaneus *in vitro* for three studies: 1. Nicholson *et al.* (2001), 2. Chaffai *et al.* (2002), and 3. the present study. 95% confidence intervals for the present study are shown in parentheses.

nBUA vs. BV/TV	0.86[1],	0.88[2],	0.85 (0.69 – 0.93)[3]
nBUA vs. BMD	-	0.84[2],	0.80 (0.61 – 0.91)[3]
phase velocity vs. BV/TV	0.86[1],	0.90[2],	0.81 (0.62 – 0.91)[3]
phase velocity vs. BMD	-	0.90[2],	0.86 (0.71 – 0.93)[3]
signal velocity vs. BV/TV	0.88[1],	-	0.77 (0.55 – 0.89)[3]
signal velocity vs. BMD	-	-	0.90 (0.80 – 0.95)[3]
backscatter coefficient vs. BV/TV	-	0.91[2],	0.84 (0.68 – 0.92)[3]
backscatter coefficient vs. BMD	-	0.89[2],	0.75 (0.52 – 0.88)[3]

Table 6.

Means, standard deviations and numbers of reported values for correlation coefficients between ultrasound parameters, BMD, and microarchitectural features from the present paper and seven other papers (Nicholson *et al.*, 1998;Trebacz and Natali, 1999;Nicholson *et al.*, 2001;Chaffai *et al.*, 2002;Hakulinen *et al.*, 2006;Padilla *et al.*, 2008;Karjalainen *et al.*, 2009).

Means	**BMD**	**BV/TV**	**BS/BV**	**Tb.Th**	**Tb.N**	**Tb.Sp**	**DA**	**SMI**
Attenuation	0.83	0.83	−0.68	0.63	0.59	−0.55	0.30	−0.74
Velocity	0.85	0.80	−0.61	0.53	0.61	−0.57	0.12	−0.69
Backscatter	0.75	0.78	−0.69	0.58	0.41	−0.47	0.38	−0.69
Std. Dev.s								
Attenuation	0.04	0.12	0.11	0.16	0.25	0.24	0.13	0.08
Velocity	0.09	0.15	0.18	0.28	0.25	0.23	0.30	0.11
Backscatter	0.14	0.11	0.16	0.18	0.50	0.37	0.26	0.20
n								
Attenuation	5	6	4	6	5	5	3	2
Velocity	5	6	4	6	5	5	3	2
Backscatter	3	5	4	5	3	5	3	2